International Journal of Heat and Mass Transfer 52 (2009) 4946–4955

Contents lists available at ScienceDirect

International Journal of Heat and Mass Transfer

journal homepage: www.elsevier.com/locate/ijhmt

Experimental study on the heat transfer characteristics during the pressure transients under supercritical pressures

Kyoung-Ho Kang [a,b,*], Soon-Heung Chang [a]

[a] Korea Advanced Institute of Science and Technology, 373-1 Guseong-Dong, Yuseong-Gu, Daejeon 305-701, Republic of Korea
[b] Thermal Hydraulic Safety Research Division, Korea Atomic Energy Research Institute, 150 Dukjin-Dong, Yuseong-Gu, Daejeon 305–353, Republic of Korea

ARTICLE INFO

Article history:
Available online 3 July 2009

Keywords:
Supercritical pressure
Pressure transient
Heat transfer rates

ABSTRACT

Main objective of this study is to investigate an applicability of a steady-state heat transfer correlation to pressure transient sequences and an effect of the pressure transient rates on the overall heat transfer rates under the supercritical pressures. Heat transfer rates are brought in line for both the pressure increasing and the pressure decreasing transients. And effects of pressure transient rates on heat transfer rates are trivial. As for an applicability of steady-state heat transfer correlation to the pressure transient sequences, the heat transfer correlation always overestimates the Nusselt number measured in the pressure transient heat transfer experiments by average 30%.

1. Introduction

SuperCritical pressure Water cooled Reactor (SCWR) is considered as one of the GEN-IV (Generation IV) innovation nuclear reactors [1]. The SCWRs, which are operated at the pressure conditions higher than the thermodynamic critical point of water (374 °C, 22.1 MPa), have advantages over the conventional water cooled reactors in terms of thermal efficiency as well as compactness and simplicity [2]. The special characteristic of fluid near the thermodynamic critical point is that their thermodynamic properties vary rapidly with temperature and pressure. A similar large variation in the fluid properties exists at a certain fluid temperature in the supercritical pressure region. The fluid temperature at which the specific heat reaches its peak value for a given pressure is known as a pseudo-critical point. The proposed designs of the SCWRs require an operation under the wide range of trans-pseudo-critical regime. Therefore, it is essential to build a reliable database on the thermal hydraulic characteristics of supercritical fluids for the operation conditions of the SCWRs.

Since supercritical pressure fluids do not undergo a change of phase, the SCWRs at the rated operating conditions are free from the critical heat flux (CHF) – related criteria. When the SCWRs are operated with a sliding pressure start-up mode [3], i.e., a nuclear heating starts at subcritical pressures, a CHF should be avoided during the power-increasing phases under subcritical pressure conditions, just as the power of Light Water Reactor (LWR) is rigidly regulated by the CHF-related criteria. Moreover, in order to ensure the reliability of safety analyses with the computer codes for abnormal pressure transients such as a loss of coolant accident, it is necessary to understand the heat transfer characteristics during the pressure transients from subcritical to supercritical pressure vice versa. The supercritical pressure fluid has already been practically utilized in the field of fossil-fired power plants and a lot of data have been accumulated since 1950s. The most previous studies, however, have been focused on the steady-state heat transfer regime to investigate the peculiar heat transfer characteristics and to develop the heat transfer coefficient. From a quantitative point of view, experimental study for the pressure transient conditions has not been performed yet.

In this study, two kinds of experiments were performed in a vertical tube of 9.4 mm inner diameter using the Freon, HFC-134a as working fluid medium to provide a reliable heat transfer database and investigate the heat transfer characteristics during the pressure transient conditions. As a reference case, the steady-state heat transfer experiments were performed under the wide range of experimental parameters which covered the mass flux from 600 to 2000 kg/m^2 s and the pressures from 4.1 to 4.5 MPa which correspond to 1.01, 1.06 and 1.11 times the critical pressure (critical pressure of the Freon, HFC-134a is 4.059 MPa), respectively. The objective of the steady-state heat transfer experiments is to examine the heat transfer characteristics and to develop a reliable heat transfer correlation which is applicable to supercritical pressure conditions.

The pressure transient heat transfer experiments were carried out for two cases of pressure increasing and decreasing transients. During the pressure transients, the mass flux, the test section inlet

* Corresponding author. Address: Thermal Hydraulic Safety Research Division, Korea Atomic Energy Research Institute, 150 Dukjin-Dong, Yuseong-Gu, Daejeon 305–353, Republic of Korea. Tel.: +82 42 868 2665; fax: +82 42 863 3689.
E-mail address: khkang@kaeri.re.kr (K.-H. Kang).

0017-9310/$ - see front matter © 2009 Elsevier Ltd. All rights reserved.
doi:10.1016/j.ijheatmasstransfer.2009.06.005

Nomenclature

c_p	specific heat (J/kg K)
D	diameter (m)
G	mass flux (kg/m^2 s)
H	enthalpy (J/kg)
h	heat transfer coefficient (W/m^2 K)
k	conductivity (W/m K)
L	length (m)
m	mass flow rate (kg/s)
n	number of data (–)
Nu	Nusselt number (–)
Re	Reynolds number (–)
Pr	Prandtl number (–)
Gr	Grashof number (–)
q''	heat flux (W/m^2)
Q	power (W)
T	temperature (K)
z	location (m)
Greeks	
ρ	density (kg/m^3)
μ	viscosity (kg/m s)
Subscripts	
exp	experiment
cal	calculation
i	inner
o	outer
w	wall
b	bulk
v	volumetric
pc	pseudo-critical

fluid temperature and the applied heat flux were held at constant values. On the basis of the test section inlet pressure, the pressures were varied from 3.8 to 4.5 MPa and vice versa in the pressure transient simulations. The pressure transient rates were varied from 1.1 to 13.6 kPa/s to evaluate the effect of the pressure transient rates on the heat transfer characteristics. Total 62 cases of the pressure transient conditions have been experimentally investigated by varying the system controlling parameters.

2. Previous works

Supercritical pressure operation is prevalent in the field of fossil-fired power plants and a lot of data have been accumulated for large-bore tubes since 1950s. At the end of the 1950s, some studies were started to investigate the applicability of supercritical pressure fluids as coolants in nuclear reactors. Several concepts of supercritical water reactor were developed from then on. Except for the erstwhile Soviet Union, however, this idea was abandoned for almost 30 years until new momentum comes into existence to adopt the SCWRs as one of the next-generation nuclear reactors in the 1990s. In this chapter, unique characteristics of heat transfer at supercritical pressures are discussed. And previous works that were done in the area of heat transfer prediction at supercritical pressures are summarized.

2.1. Heat transfer characteristics of supercritical pressure fluid

The special feature of fluid at supercritical pressures is that their thermodynamic properties vary rapidly with temperature and pressure. Fig. 1 shows the thermophysical property variations according to the temperatures for supercritical pressure water at 25.0 MPa. All thermophysical properties undergo significant changes near the pseudo-critical point as shown in Fig. 1. The specific heat rises sharply to a peak value and then falls steeply. Density and dynamic viscosity undergo a significant drop within a very narrow temperature range in the vicinity of the pseudo-critical temperature. In related with the thermophysical property variations with the temperatures, other fluids such as CO_2 and HFC-134a follow the similar trends with supercritical pressure water. In general, as pressure is increased, the pseudo-critical temperature increase and the maximum value of the specific heat decreases and the variations of the other properties with temperature become less severe. This strong dependence of thermodynamic properties on temperature and pressure leads to different heat transfer regime according to a small change of fluid temperature.

At supercritical pressure, despite non-existence of tangible phase change, the working fluid undergoes a transition form liquid-like substance to gas-like one without any of discontinuities associated with two phases being present when the fluid temperature rises up and passes the pseudo-critical temperature. Depending on the applied heat flux and the mass flux of flow, the heat transfer regime can be categorized into three types of enhanced, normal and deteriorated heat transfer at supercritical pressure. In general, deviations from normal heat transfer have been found to occur when the wall temperature is greater than the pseudo-critical temperature and the bulk fluid temperature is less than the pseudo-critical temperature, i.e., $T_w > T_{pc} > T_b$. This criterion indicates the condition of large property variations occurring within the near wall region.

Impairment of heat transfer, i.e., heat transfer deterioration can be induced by the combined effects of heat flux and mass velocity in the vertically upward flow. In case of high heat flux, turbulence is reduced as a result of the thermal acceleration due to heating and the consequent density reduction of the fluid. Turbulent diffusivity is reduced when the low-density wall layer becomes thick enough to reduce the shear stress brought about by flow acceleration due to heating. In case of low mass flux, buoyancy force accelerates the flow velocity near the wall. This makes the flow velocity distribution to be flat and turbulence energy generation is reduced.

2.2. Prediction methods for forced convective heat transfer of supercritical pressure fluid

Radial variations of the thermophysical properties near the wall with the temperatures result in the complexities of the heat transfer behavior at the supercritical pressure fluid. Therefore, a convective heat transfer correlation for a constant property fluid such as the well-known Dittus–Boelter correlation is no longer applicable to the supercritical pressure fluid. In related with the prediction methodology, satisfactory analytical models have not yet been developed due to the difficulty in dealing with the rapid variations of fluid thermophysical properties. Therefore, empirical correlations based on experimental data are usually adopted for calculation of heat transfer rates at supercritical pressure conditions.

Various correlations have been developed for the normal heat transfer, based on the experimental data of water, carbon dioxide, and the Freon. Most of these correlations are expressed in the form of a constant properties heat transfer correlation multiplied by the

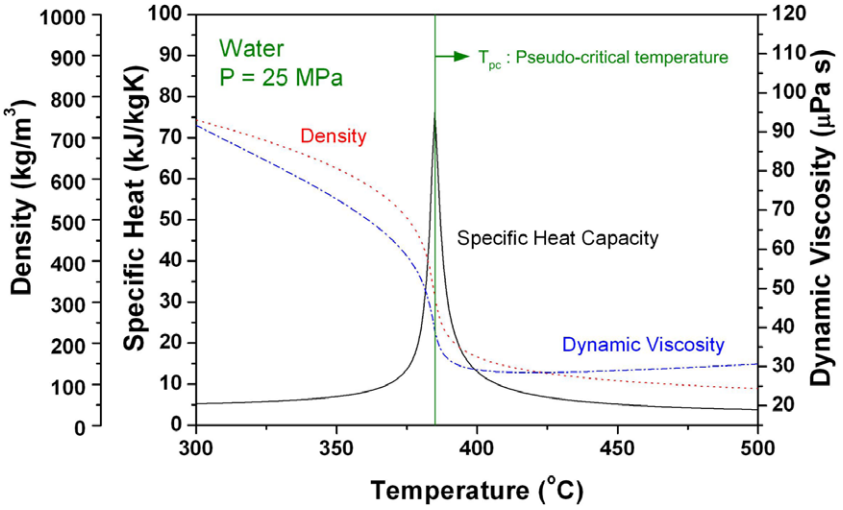

Fig. 1. Thermophysical property variations according to temperatures for supercritical pressure water at 25.0 MPa.

ratios of properties between the bulk fluid temperature and the wall temperature. Of the available heat transfer correlations, representative and reliable ones are introduced in this paper.

Bishop et al. [4] carried out experiments for supercritical water flowing upward inside tube and annuli within the following range of flow and operating parameters: pressure 22.8–27.6 MPa, bulk fluid temperature 282–527 °C, mass flux 651–3662 kg/m^2 s and heat flux 0.31–3.46 MW/m^2. The following Bishop correlation has been found to correlate their data with an accuracy of ±15%. Bishop considered the entrance effect in the heat transfer correlation.

$$Nu = \frac{hD}{k_b} = 0.0069 Re_b^{0.9} \overline{Pr}_b^{0.66} \left(\frac{\rho_w}{\rho_b}\right)^{0.43} \left(1 + 2.4\frac{D}{x}\right) \quad (1)$$

In 1979, Jackson and Hall [5] discussed about the predicting performance of the existing correlations using approximately 2000 experimental data for water and carbon dioxide, and concluded that the Krasnoshchekov correlation [6] showed the best predicting performance. Jackson and Hall proposed a modified form of the Krasnoshchekov correlation as follows:

$$Nu = \frac{hD}{k_b} = 0.0183 Re_b^{0.82} Pr_b^{0.5} \left(\frac{\rho_w}{\rho_b}\right)^{0.3} \left(\frac{\overline{c_p}}{c_{pb}}\right)^{n} \quad (2)$$

$$n = 0.4 \quad \text{for } T_b < T_w < T_{pc} \quad \text{and} \quad 1.2T_{pc} < T_b < T_w$$

$$n = 0.4 + 0.2\lfloor (T_w/T_{pc}) - 1 \rfloor \quad \text{for } T_b < T_{pc} < T_w$$

$$n = 0.4 + 0.2\lfloor (T_w/T_{pc}) - 1 \rfloor \{1 - 5\lfloor (T_b/T_{pc} - 1) \rfloor\}$$
$$\text{for } T_{pc} < T_b < 1.2T_{pc} \quad \text{and} \quad T_b < T_w$$

Furthermore, Jackson and Fewster [7] proposed a simplified form of the modified Krasnoshchekov correlation by employing constant index of the thermophysical property ratios as follows. This correlation is similar to the Bishop correlation without the effect of geometrical parameters and with different values of constant and exponents.

$$Nu = \frac{hD}{k_b} = 0.0183 Re_b^{0.82} \overline{Pr}_b^{0.5} \left(\frac{\rho_w}{\rho_b}\right)^{0.3} \quad (3)$$

Recently, new type correlations were proposed by considering the effect of buoyancy on the heat transfer rates. Buoyancy effect driven by the abrupt density difference between near the wall and center of the tube is one of the important parameters controlling the heat transfer characteristics at supercritical pressure. As for the normal heat transfer regime, Watts et al. [8] developed a heat transfer correlation for the vertically upward flowing supercritical pressure water as follows:

$$Nu = Nu_{var\,P} \left[1 - \frac{3000\overline{Gr}_b}{Re_b^{2.7}\overline{Pr}_b^{0.5}}\right]^{0.295} \quad \text{for } \frac{\overline{Gr}_b}{Re_b^{2.7}\overline{Pr}_b^{0.5}} < 10^{-4} \quad (4)$$

$$Nu = Nu_{var\,P} \left[\frac{7000\overline{Gr}_b}{Re_b^{2.7}\overline{Pr}_b^{0.5}}\right]^{0.295} \quad \text{for } \frac{\overline{Gr}_b}{Re_b^{2.7}\overline{Pr}_b^{0.5}} > 10^{-4}$$

where $Nu_{var\,P} = 0.021 Re_b^{0.8} \overline{Pr}_b^{0.55} \left(\frac{\rho_w}{\rho_b}\right)^{0.35}$

As for the Watts correlation, Komita et al. [9] modified the equation for deteriorated heat transfer and found their HCFC-22 experimental data to be predicted in ±20% of error range. In the Watts and the Komita correlations, the criteria term is the buoyancy parameter which was driven by Jackson and Hall.

Although these correlations have been found to predict reasonably well for their original experimental data, large deviations can not be avoided in estimating the heat transfer rates for the different operating conditions such as fluids, geometry, and system parameters and so on. These deviations could be attributed to the complicated heat transfer characteristics of the supercritical pressure fluids and poor understanding of heat transfer impairment phenomena.

2.3. Safety analysis for abnormal transients of SCWRS

As the detailed design of the SCWRs is consolidated, some efforts are being made to perform a safety analysis for abnormal transients of the SCWRs, recently. Ishiwatari et al. [10] performed the safety analysis for the SCWR concept developed by University of Tokyo. They used SPRAT code as a safety analysis tool. As for heat transfer model between the core and the supercritical pressure water, Jones and Launder k–e model is adopted in the SPRAT code. Through the safety analysis they insisted that the SCWR concept has a sufficient safety margin.

Dumaz et al. [11] extended the applicability of the CATHARE2 code above the critical point of water and performed a preliminary assessment. They simulated the loss of coolant accidents considering simple sequences of events. As a first step of the safety analysis for the SCWRs, they adopted the Dittus–Boelter correlation as a heat transfer correlation between the core and the supercritical

pressure water. By performing the preliminary studies, they insisted that the CATHARE2 code has the potential to be used as a reliable safety analysis tool for the SCWRs.

Jaeger et al. [12] checked the appropriateness of TRACE code for safety studies of systems with supercritical water. They performed the post-test calculation of the Yamagata experiment. They modified the TRACE code by implementing new correlations for the transport properties such as dynamic viscosity and thermal conductivity. And also they implemented several open-literature heat transfer correlations which are applicable to the supercritical pressure fluids. Despite the preliminary assessments, they insisted that the modified TRACE version is now able to handle supercritical conditions.

The present safety analyses for abnormal transients of SCWRs are rather premature. Until now, efforts are being focused on the extension of the applicability of the existing computer codes to the supercritical pressure fluids. Preliminary assessment results suggest the improvement of the physical models, in particular, the heat transfer correlation at supercritical pressure conditions. As a further study, they highly recommend the detailed investigation on the pressure transient heat transfer from subcritical to supercritical pressures to have better confidence in the safety analysis result using the computer codes.

3. Description of experiments

3.1. Experimental facility and measurements

For investigation of the heat transfer characteristics at supercritical pressures, experiments were performed using the Freon Thermal Hydraulic Experimental Loop (FTHEL) [13]. The FTHEL facility consists of a closed hydraulic loop with two non-seal canned motor pump connected in a series, a flow meter, two pre-heaters, an inlet throttling valve, a test section, a condensing and cooling system. Fig. 2 shows the schematic diagram of the FTHEL facility. The system was designed with operating limits of 4.5 MPa and 150 °C. The tests were conducted in a vertical tube of 9.4 mm inner diameter using the Freon, HFC-134a as working fluid medium. The Freon, HFC-134a is adopted as a modeling fluid since it has a much lower critical temperature and pressure than water and shows similar changes in its thermodynamic properties near a pseudo-critical temperature.

The test section is uniformly heated in axial direction and heating length is 2000 mm. In the experiments, wall temperature of the test section is primary measurement parameter for evaluating the heat transfer characteristics at supercritical pressures. The outer wall temperature variations along the test section are measured by Chromel-alumel sheath type thermocouples. The sheath diameter of the thermocouples is 0.5 mm and they are electrically insulated. Thirty-nine thermocouples are silver-soldered to outer wall of the test section with spacing of 50 mm. The test section is thermally insulated with ceramic wool and wrapped by ceramic tape in order to minimize a heat loss during the experiments. Fig. 3 shows the schematic diagram and the photograph of the vertically mounted test section.

Fluid temperature at the inlet and the outlet of the test section are measured by calibrated platinum resistive thermometers (RTD). And also T-type thermocouples of Copper–Constantan are installed for complementary measurement. The thermocouples are connected to the data acquisition system and processed by the data acquisition system. Pressure measurements are made at the inlet and the outlet of the test section and the loop of the FTHEL facility. Smart type pressure transmitters manufactured by Rosemount are used for the measurement of pressure. Flow rate is measured with U-tube type mass flow meter having accuracy of ±0.2%, which was manufactured by Micro Motion.

The DC power applied to the test section is measured by means of voltage and current readings. Voltage drops are directly measured by an integral voltmeter by means of two copper wires connected at both ends of the copper power clamps in the test section. For measuring the electric current, a shunt with ±0.5% of accuracy is installed between the main power line and the test section, and it measures the DC up to 15,000 A.

3.2. Experimental procedure and conditions

Before starting a set of main experiments, a heat balance test under single phase flow condition is carried out to estimate the heat loss from the test section and to check a proper working of the test section instrumentation. In the heat balance tests, under

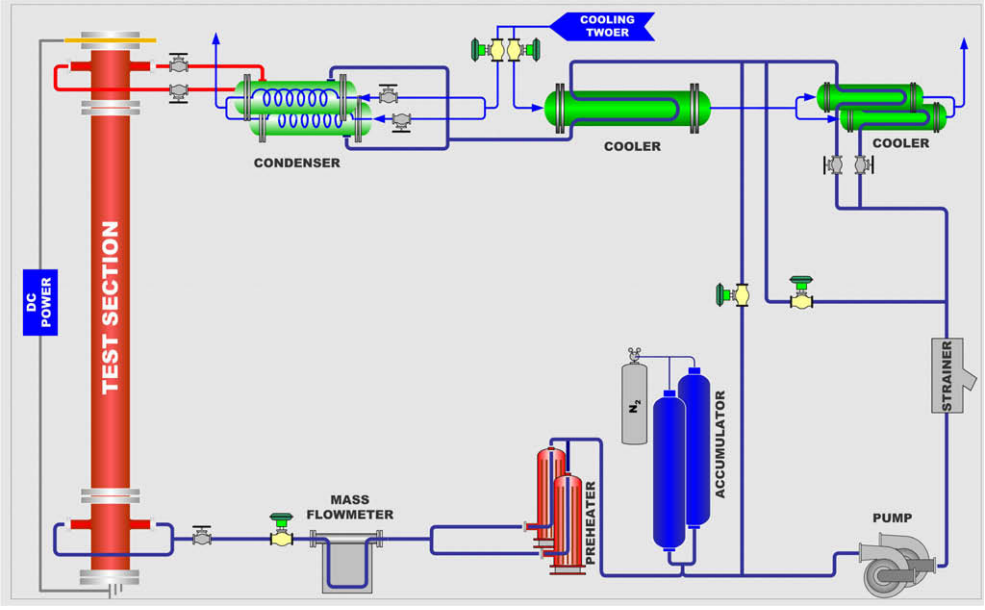

Fig. 2. Schematic diagram of the FTHEL facility.

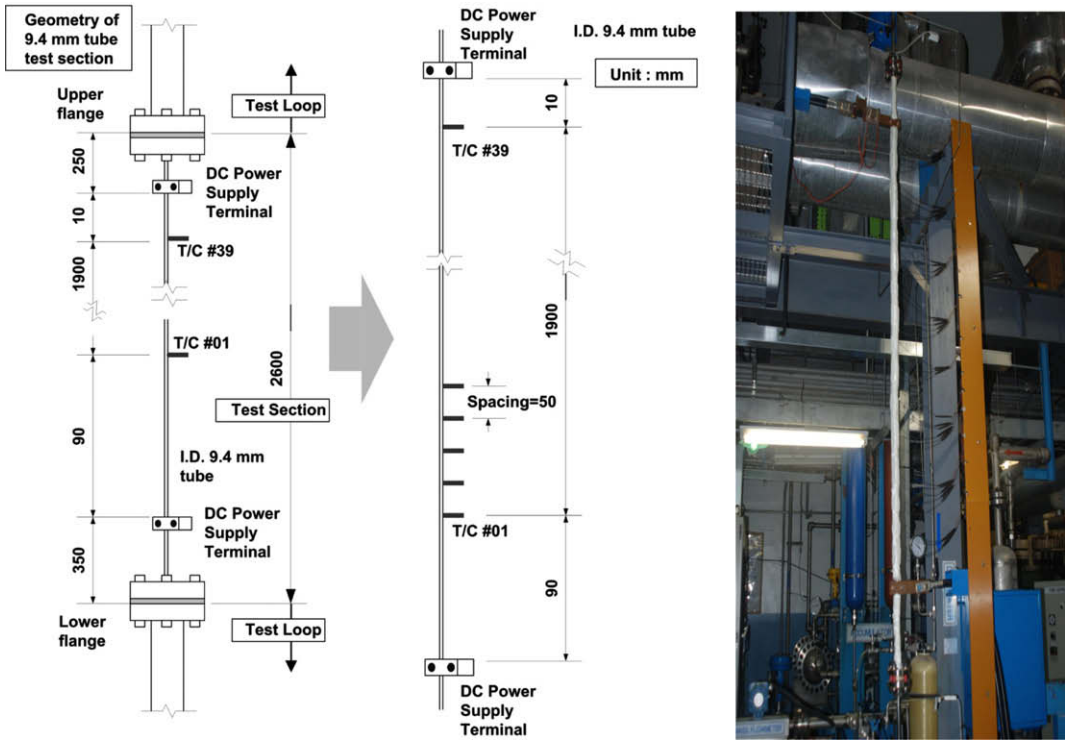

Fig. 3. Schematic diagram and photograph of the test section.

the specific test conditions of test section inlet pressure, inlet temperature, and mass flow rate, total power applied to the test section is compared with the enthalpy rise of fluid through the test section. Actually, the heat loss was very less than ±1% in this study.

Before getting the data acquisition, the system conditions such as inlet pressure, inlet fluid temperature, inlet mass flux, and applied heat flux were maintained to the desired values of experimental conditions. In case of steady-state heat transfer experiment, data were measured and recorded for about 300 s after achieving nearly constant system conditions and the parameters were averaged for total 200 data. In case of pressure transient heat transfer experiment, the pressure transients were controlled using accumulators at the desired pressure transient rates.

The steady-state heat transfer experiments have been performed with various heat and mass fluxes at a fixed pressure. The mass flux was in the range between 600 and 2000 kg/m^2 s and the maximum heat flux was 160 kW/m^2. The selected pressures were 4.1, 4.3 and 4.5 MPa which correspond to 1.01, 1.06 and 1.11 times the critical pressure (critical pressure of the Freon, HFC-134a is 4.059 MPa), respectively. Total number of data obtained from the steady-state heat transfer experiments are about 8300 for the various regime of heat transfer including normal, enhanced and deteriorated mode.

The pressure transient heat transfer experiments have been carried out for two cases of pressure increasing and decreasing transients. During the pressure transients, the mass flux, the test section inlet fluid temperature and the heat flux were held at constant values. On the basis of the test section inlet pressure, the pressures were varied from 3.8 to 4.5 MPa and vice versa in the pressure transient simulations. The mass flux was in the range between 600 and 2000 kg/m^2 s and the heat flux was in the range between 10 and 140 kW/m^2. The pressure transient rates were varied from 1.1 to 13.6 kPa/s to evaluate the effect of the pressure transient rates on the heat transfer characteristics. Total 62 cases of the pressure transient conditions have been experimentally investigated by varying the system controlling parameters. Table 1 summarizes the detailed experimental conditions.

3.3. Data reduction

To develop the heat transfer correlation, heat transfer rates from the inner wall of the test section to the fluid should be evaluated from the measured parameters in the steady-state heat transfer experiment. The local heat transfer coefficient can be defined as follows:

$$h = q''/(T_{w,z} - T_{b,z}) \tag{5}$$

The heat flux at the inner surface of the tube can be determined by dividing the total applied power by the heated area. The total applied power is the product of voltage and current imposed by the power supply system.

$$q'' = \dot{Q}/(\pi D_i L_H) = (VI)/(\pi D_i L_H) \tag{6}$$

In the experiments, the local fluid temperature did not be directly measured for avoiding the flow obstruction in the tube having a narrow inner diameter of 9.4 mm. Instead of direct measurement, the local fluid temperature can be obtained with the assumption that the specific enthalpy of the fluid increases linearly with axial locations in case of uniform heat flux conditions.

$$H_{b,z} = H_{b,in} + [(z - z_o)/L_H] \cdot (\dot{Q}/\dot{m}) \tag{7}$$

The local fluid temperature can be calculated from thermophysical properties of specific enthalpy and system pressure as follows:

$$T_{b,z} = f(H_{b,z}, P_{in}) \tag{8}$$

Since the inner wall temperature can not be directly measured in the experiment, the temperature at the inner surface should be calculated from the measured value at the outer wall by using a heat conduction model of cylindrical tube in case of a uniform heat generation as follows:

Table 1
Experimental conditions.

Experiment	Inlet pressure (kPa)	Inlet temperature (°C)	Heat flux (kW/m^2)	Mass flux (kg/m^2 s)	No. of data (–)
Steady-state experiment	4100, 4300, 4500	50–110	10–160	600–2000	8300
Pressure transient experiment	3800–4500	91	10–140	600–2000	62 cases

$$T_{w,i} = T_{w,o} + \frac{\dot{q}_v}{4k_w}\left[\left(\frac{D_o}{2}\right)^2 - \left(\frac{D_i}{2}\right)^2\right] - \frac{\dot{q}_v}{2k_w}\left(\frac{D_o}{2}\right)^2 ln\frac{D_o}{D_i} \quad (9)$$

where $\dot{q}_v = \dot{Q}/\left[\frac{\pi}{4}(D_o^2 - D_i^2)L_H\right]$: volumetric heat generation.

By substituting q'', $T_{b,z}$ and $T_{w,z}$ from Eqs. (6), (8), (9) into Eq. (5), the local heat transfer correlation is obtained in this study.

3.4. Uncertainty analysis

Every measurement always includes error which results in a difference between the measured value and the true value. The difference between the measured value and the true value is the total measurement error. Since the true value or the error is unknown and unknowable, its limits must be estimated at a given confidence. This estimate is called the uncertainty. In 1993, The International Standard Organization (ISO) published the "Guide to the Expression of Uncertainty in Measurement (GUM)" in the name of seven international organizations, which formally established general rules for evaluating and expressing uncertainty in measurement. This guide was corrected and reprinted in 1995 and usually referred to simply as the GUM [14].

The uncertainties of the measurements were estimated from the calibration of the sensors and the accuracy of the equipments according to the ISO GUM method with a coverage factor of 1.96 and a confidence level of 95%. Table 2 summarizes the results of the uncertainty analysis for the major experimental parameters.

4. Experimental results and discussions

4.1. Steady-state heat transfer experiments

In the steady-state heat transfer experiments, major experimental parameters are heat flux, mass flux, inlet fluid temperature and inlet system pressure. Fig. 4 show variation of the wall temperatures and the heat transfer coefficients against the bulk fluid enthalpy with a parameter of heat flux at the mass flux of 600 kg/m^2 s. The wall temperature is the temperature at the inner wall of the tube calculated by Eq. (9). In these figs, several data sets which were obtained at different inlet fluid enthalpies with a fixed value of heat flux, mass flux and inlet pressure are plotted together. The black solid line is the calculated bulk fluid temperature and the enthalpy at the pseudo-critical temperature (H_{pc}) is denoted as a red dotted line in each figure.

Fig. 4 represents typical patterns of the temperatures and the heat transfer coefficients during the steady-state heat transfer experiments. According to Fig. 4, thermal behavior of the tube is determined mainly by the applied heat flux and the mass flux of

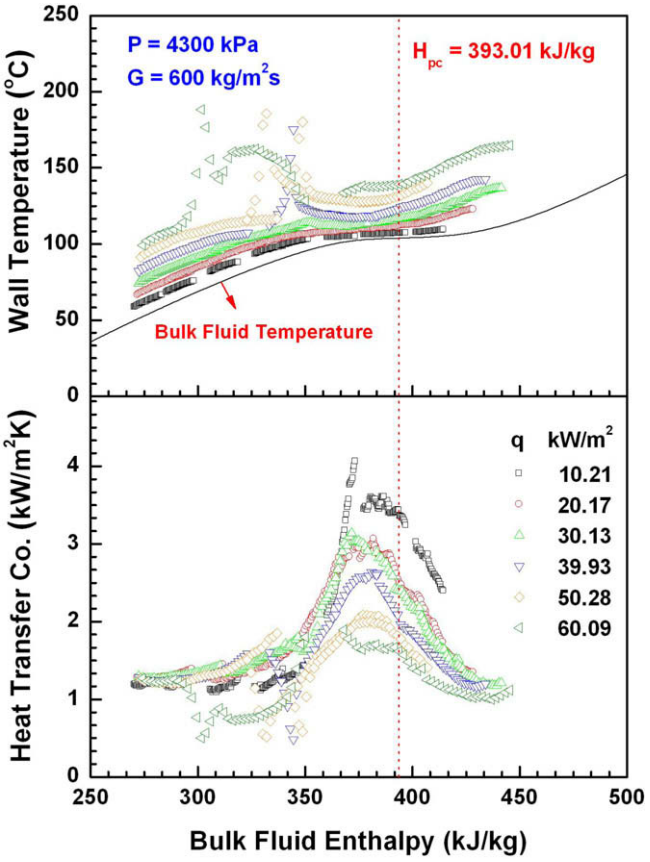

Fig. 4. Variation of wall temperature and heat transfer coefficient: P = 4300 kPa, G = 600 kg/m^2 s.

fluid, which shows a general agreement with findings of previous studies and understandings. In case of a low heat flux, wall temperature profile is parallel to bulk fluid temperature line, and the heat transfer coefficient has the maximum value at slightly lower than a pseudo-critical enthalpy. The wall temperature, however, shows abrupt increase with increase of a heat flux, which clearly indicates the occurrence of heat transfer deterioration. As a heat flux is increased, starting time for heat transfer deterioration has a tendency to be earlier.

Experimental data on forced convection of the steady-state heat transfer are correlated in terms of dimensionless parameters for the purpose of design calculations and safety analysis in the

Table 2
Results of uncertainty analysis.

Parameters	Instruments	Nominal value	Relative uncertainty (%)
Tube outer wall temperature	K-type thermocouples	200 °C	0.88
Inlet and outlet fluid temperature	RTD	150 °C	0.37
Pressure	Rosemount smart type	4500 kPa	0.18
Mass flux	Coriolis mass flow meter	1250 kg/m^2 s	1.52
Heat flux	Shunt, voltmeter	160 kW/m^2	1.20
Heat transfer coefficient	Evaluation	5 kW/m^2 K	3.68

SCWRs. For forced convection flow under conditions where the influence of buoyancy, compressibility and dissipation are negligible, the local Nusselt number can be derived with the functional dependence as follows [5]:

$$Nu_b = f\lfloor Re_b, Pr_b, x/d, \rho_w/\rho_b, \mu_w/\mu_b, c_{pw}/c_{pb}, k_w/k_b \rfloor \quad (10)$$

Therefore, heat transfer correlations can be expressed in the form of a constant properties heat transfer correlation multiplied by the ratios of properties between the bulk fluid temperature and the wall temperature. Among the various properties, specific heat is the most influencing parameter in heat transfer rate under the supercritical pressure. In order to take account of abrupt variation of specific heat with temperatures, an integrated specific heat ($\overline{c_p}$) and Prandtl number ($\overline{Pr}$) are employed assuming constant pressure as follows:

$$\overline{c_p} = \frac{1}{T_w - T_b}\int_{T_b}^{T_w} c_p dT = (H_w - H_b)/(T_w - T_b) \quad (11)$$

$$\overline{Pr} = \frac{\mu_b \overline{c_p}}{k_b} \quad (12)$$

Heat transfer correlation was developed considering the properties variation near the wall. The proposed correlation given by Eq. (13) predicts the Nusselt number within ±20% accuracy for the 94.6% of present experimental data for the normal heat transfer regime. The total data point is 7022. Fig. 5 shows the comparison of experimental and estimated data for the Nusselt number.

$$Nu_b = 0.0244 Re_b^{0.762} \overline{Pr}^{0.552} \left(\frac{\rho_w}{\rho_b}\right)^{0.0293} \quad (13)$$

For a quantitative comparison of the deviation between the experimental and correlated heat transfer coefficients, RMS (Root-Mean-Square) deviation and mean deviation of the prediction error are calculated as follows. RMS deviation and mean deviation are 0.106 and 0.0006, respectively.

$$\varepsilon_{RMS} = \sqrt{\frac{1}{n}\sum\left(\frac{Nu_{ccal} - Nu_{exp}}{Nu_{exp}}\right)^2} \quad (14)$$

$$\bar{\varepsilon} = \frac{1}{n}\sum\left(\frac{Nu_{ccal} - Nu_{exp}}{Nu_{exp}}\right) \quad (15)$$

The proposed heat transfer correlation was tested against the experimental data of open literature. For a reference, the experiments performed by Yamagata et al. [15], Lee et al. [16], Komita et al. [9], Pioro et al. [17] and Kim et al. [18] are selected. Fig. 6 shows the comparison of experimental and estimated data for the Nusselt number. The total data point is 1073 and the proposed correlation predicts the Nusselt number within ±20% accuracy for the 86.4% of the selected experimental data which were obtained using water, R-22 and CO_2. RMS deviation and mean deviation of the prediction error are 0.098 and −0.035, respectively. This statistical result indicates that the proposed heat transfer coefficient is plausibly applicable to the different experimental conditions and the other working fluids of supercritical pressures.

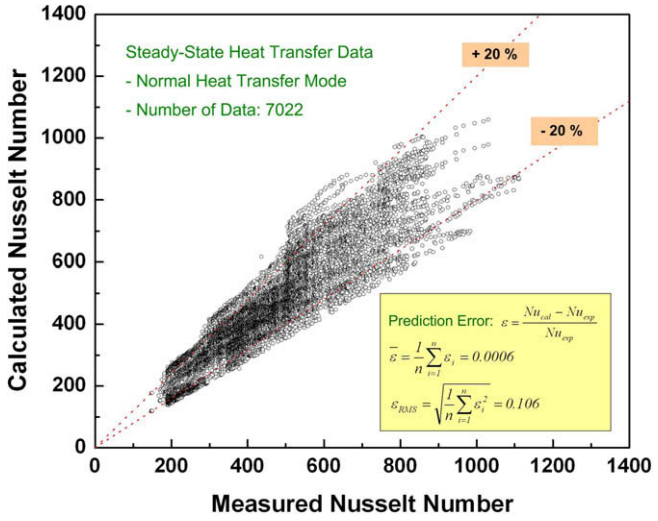

Fig. 5. Comparison of experimental and estimated data for the Nusselt number.

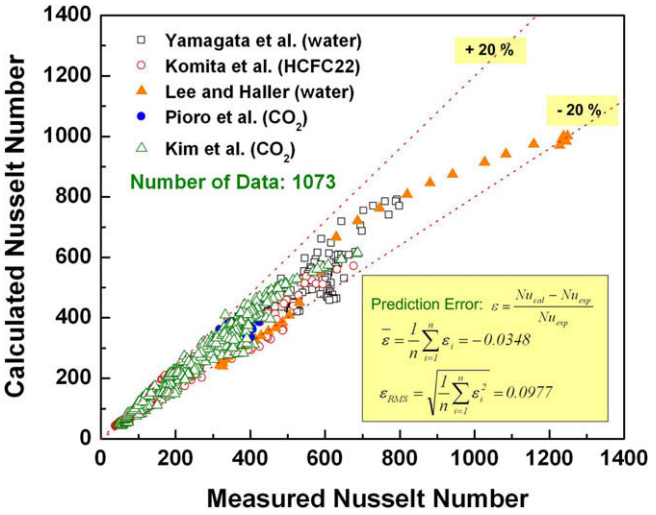

Fig. 6. Test result of heat transfer correlation against the experimental data of open literature.

4.2. Pressure transient heat transfer experiments

In order to ensure the reliability of safety analyses with the computer codes for abnormal pressure decreasing transients including a loss of coolant accident, it is necessary to understand the heat transfer characteristics during the pressure transients from subcritical to supercritical pressure vice versa. During the pressure transients, the mass flux, the test section inlet fluid temperature and the heat flux were held at constant values. On the basis of the test section inlet pressure, the pressures were varied from 3.8 to 4.5 MPa and vice versa in the pressure transient simulations.

Fig. 7 shows the variation of the wall temperatures during the pressure increasing and the pressure decreasing transients for a fixed heat and mass flux, respectively. In Fig. 7, the notation of thermocouple location is edited out for simplified expression of the overall thermal behavior because 39 thermocouples are installed at the test section. Near the critical pressure, the heat transfer mode is most remarkably changed at reduced pressure (P/P_c) ranging from 0.97 to 0.99. In the pressure increasing transient, the upper part of the test section maintains the stable post-CHF heat transfer at subcritical pressure region and the lower part of the test section experiences the occurrence of CHF as pressure approaches the critical pressure. Compared to the CHF and the post-CHF situation of the subcritical pressure, enhanced heat transfer is dominant under the supercritical pressure as shown in Fig. 7. In the pressure decreasing transient, as soon as the pressure decreases to the subcritical pressure, wall temperatures abruptly jump, which can be characterized as a CHF phenomenon.

During the pressure transients, the specific volume of high temperature coolant above the critical point increase continuously as the system pressure decreases from the supercritical to subcritical region. Slightly above the critical pressure, supercritical fluid is

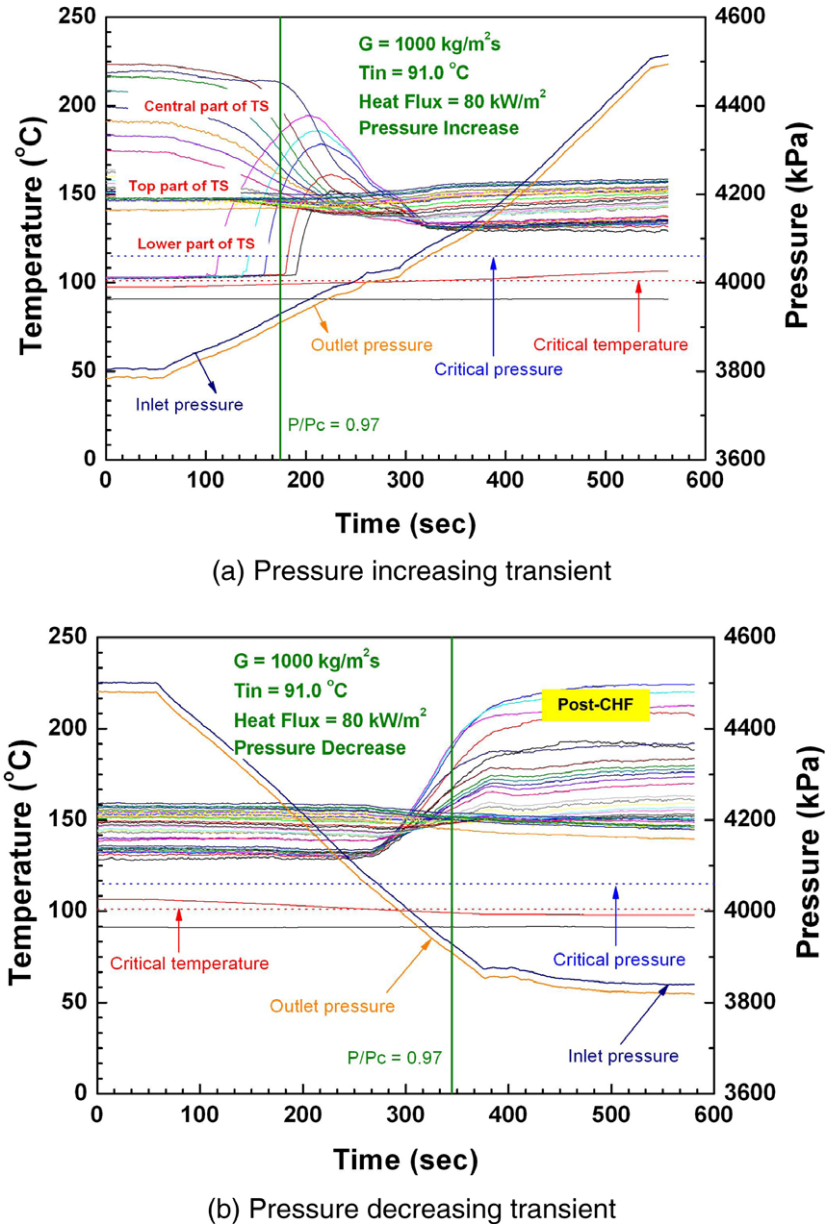

Fig. 7. Variation of wall temperature during pressure transients.

dense, highly heat conducting and deep heat reservoirs at constant pressure. And it is also poorly heat diffusing and highly expandable medium. These peculiar characteristics of near critical fluid may affect the abrupt change of heat transfer mode during the pressure transients.

From a quantitative point of view, heat transfer rates are brought in line for both the pressure increasing and the pressure decreasing transients under the supercritical pressure region as shown in Fig. 8. Pressure transient rates during postulated loss of coolant accident in the SCWRs can be varied according to the break size and accident sequences. For mild transient of loss of coolant accident, the pressure transient rate is around 10 kPa/s [10]. In this study, effects of pressure transient rates on the heat transfer characteristics are examined during the pressure transients. The pressure transient rates range from 1.1 to 13.6 kPa/s in the present experimental conditions. Fig. 9 shows the variation of heat transfer coefficients against pressure transient rates for a given heat flux and mass flux. Under the supercritical pressures, variations of heat transfer rates according to the pressure transient rates are trivial in both the mass flux of 600 and 1000 kg/m^2 s.

From a safety analysis point of view, the applicability of steady-state heat transfer correlation for the pressure transient conditions is one of the most important pending issues in that heat transfer correlation developed from the steady-state heat transfer experiment is directly adopted in the most safety analysis codes. In this study, the applicability of steady-state heat transfer correlation for the pressure transient sequences is evaluated. Fig. 10 shows the comparison of experimental and calculated data for the Nusselt number via applying the steady-state heat transfer correlation to the data of pressure transient heat transfer experiments. It could be found from Fig. 10 that the steady-state heat transfer correlation developed using the steady-state heat transfer experimental data overestimates the Nusselt number measured in the pressure transient heat transfer experiments by 10–40%. During the pressure transients, the wall temperature and the bulk fluid temperature do not change significantly for a fixed heat flux level as

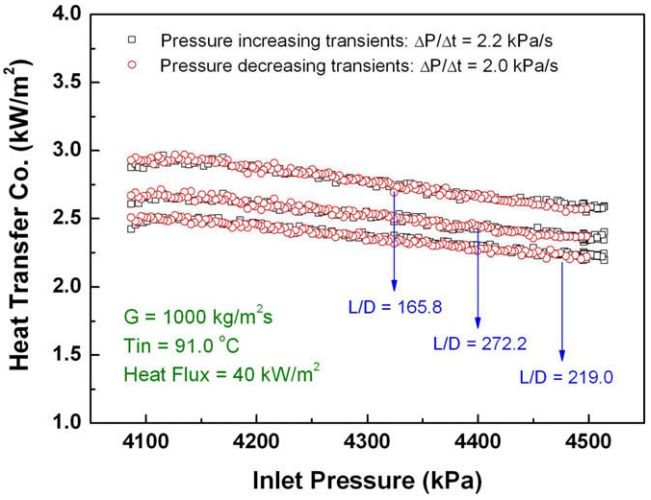

Fig. 8. Comparison of heat transfer coefficients between the pressure increasing and the pressure decreasing transients.

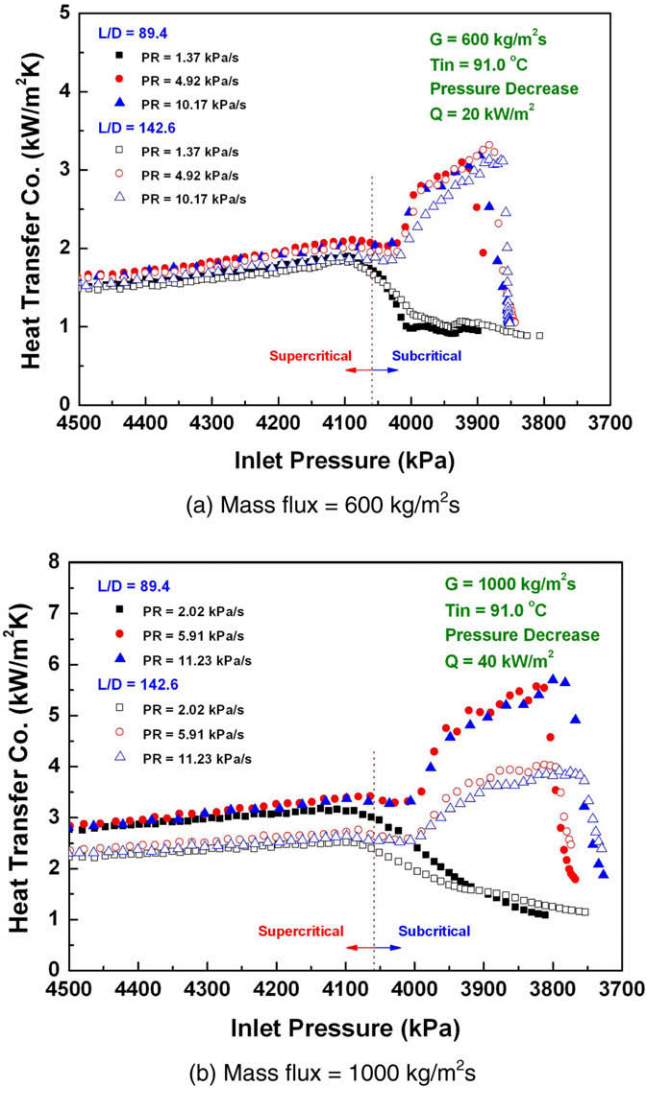

Fig. 9. Variation of heat transfer coefficient against pressure transient rates.

shown in Fig. 11. An individual term of the heat transfer correlation, however, is a function of system conditions and they are

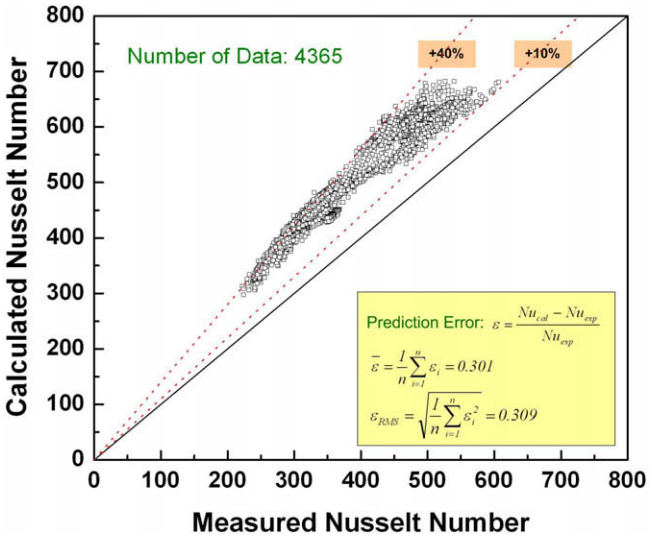

Fig. 10. Test results for applicability of the steady-state heat transfer correlation to the pressure transient conditions.

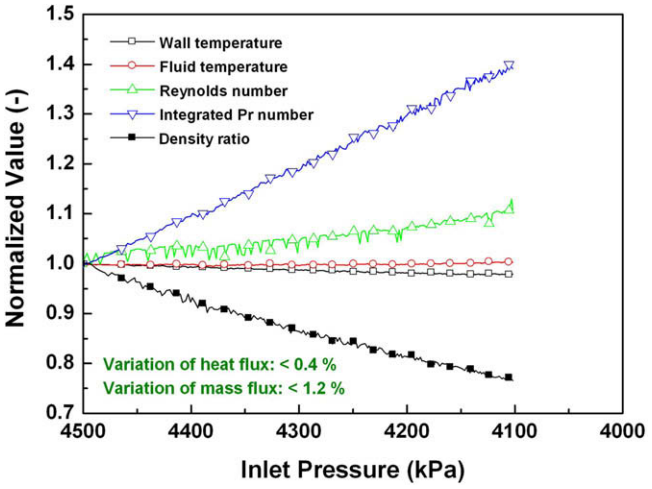

Fig. 11. Variation of individual term of the heat transfer correlation during the pressure transients.

highly dependent on system parameters, especially the pressure. Especially, increase of integrated Prandtl number is remarkable during the pressure decreasing transient. Therefore, the steady-state heat transfer correlation consistently overestimates the heat transfer rates during the pressure transients as shown in Fig. 10.

5. Conclusions

Experiments were performed in a vertical tube of 9.4 mm inner diameter using the Freon, HFC-134a as working fluid medium under the supercritical pressure range. Two kinds of experiments, i.e., steady-state and pressure transient, were carried out. As for the steady-state heat transfer experiment, the selected pressures were 4.1, 4.3 and 4.5 MPa which correspond to 1.01, 1.06 and 1.11 times the critical pressure, respectively. The inlet pressures were varied from 3.8 to 4.5 MPa and vice versa in the pressure transient simulations. Through the steady-state heat transfer experiment, heat transfer correlation is suggested. And also heat transfer characteristics during the pressure transients are examined and the applicability of steady-state heat transfer correlation for the pressure

transient conditions is evaluated. Some insights gained from the present study include:

- Parametric trends of the heat transfer characteristics of the supercritical pressure fluid show a general agreement with findings of previous studies and understandings. Heat transfer correlation was developed considering the properties variation near the wall. The proposed correlation predicts the Nusselt number within ±20% accuracy for the 94.6% of present 7022 experimental data point. Test results against the experimental data of open literature obtained using water, HCFC-22 and CO_2 indicate good predicting capability of the proposed correlation.
- During the pressure transients, near the critical pressure, the heat transfer mode is most remarkably changed at reduced pressure (P/P_c) ranging from 0.97 to 0.99. Compared to the CHF and the post-CHF situation of the subcritical pressure, enhanced heat transfer is dominant under the supercritical pressure.
- From a quantitative point of view, heat transfer rates are brought in line for both the pressure increasing and the pressure decreasing transients under the supercritical pressure region.
- During the pressure decreasing transients, heat transfer rates increased slightly compared to those of initial values at 4500 kPa, which could be attributed to the dominant peak value of specific heat with a decrease in pressure. However, variations of heat transfer rates according to the pressure transient rates are trivial in all the experimental conditions.
- The applicability of steady-state heat transfer correlation for the pressure transient sequences is evaluated. The steady-state heat transfer correlation developed using the steady-state heat transfer experimental data always overestimates the Nusselt number measured in the pressure transient heat transfer experiments by 10–40%.

As for the applicability of steady-state heat transfer correlation to the pressure transient sequences, the steady-state heat transfer correlation developed using the steady-state heat transfer experimental data always overestimates the Nusselt number measured in the pressure transient simulations by 10–40%. From a safety analysis point of view, it is highly recommended that sufficient thermal margin up to 40% should be considered for the safety analysis of pressure transient sequences of the SCWRs.

Acknowledgements

This work was supported by Nuclear Research & Development Program of the Korea Science and Engineering Foundation (KOSEF) grant funded by the Korean government (MEST) (Grant Code: M20702040003-08M0204-00310). The authors would like to be grateful for the technical support by Mr. Youn, Young-Jung and Mr. Park, Jong-Kuk in Korea Atomic Energy Research Institute (KAERI).

References

[1] Y. Oka, S. Koshizuka, Design concept of once-through cycle supercritical-pressure water cooled reactors, in: Proceedings of SCR-2000: The First International Symposium on Supercritical Water-Cooled Reactors, Design and Technology, Tokyo, Japan, 2000, pp. 1–22.
[2] S.Y. Chun et al., Critical heat flux in a heater rod bundle cooled by R-134a fluid near the critical pressure, J. Nucl. Sci. Technol. 44 (9) (2007) 1189–1198.
[3] H.W. Byeon et al., Designing a standard thermal power plant for daily startup/shutdown: the HP bypass control and safety function, ISA Trans. 36 (1997) 71–77.
[4] A.A. Bishop et al., Forced Convection Heat Transfer to Water at Near-Critical Temperatures and Super-Critical Pressures, WCAP-2056, Westinghouse Electric Cooperation, 1964.
[5] J.D. Jackson, W.B. Hall, Forced convection heat transfer to fluids at supercritical pressure, in: Turbulent Forced Convection in Channels and Bundles, vol. 2, Hemisphere, New York, 1979, pp. 563–611.
[6] E.A. Krasnoshchekov et al., Experimental study of heat exchange in carbon dioxide in the supercritical range at high temperature drops, Teplofiz. Vys. Temp. 4 (1966) 389–398.
[7] J.D. Jackson, J. Fewster, Forced Convection Data for Supercritical Pressure Fluids, HTFS 21540, 1975.
[8] M.J. Watts et al., Mixed convection heat transfer to supercritical pressure water, in: Proceedings of Seventh International Heat Transfer Conference, Munchen, 1982, pp. 495–500.
[9] H. Komita et al., Study on the heat transfer to the supercritical pressure fluid for supercritical water cooled power reactor development, in: Proceedings of NURETH-10, Seoul, Korea, 2003.
[10] Y. Ishiwatari et al., Safety design principle of supercritical water cooled reactor, in: Proceedings of ICAPP'04, Pittsburgh, PA, USA, 2004.
[11] P. Dumaz et al., The extension of the CATHARE2 computer code above the critical point, applications to a supercritical light water reactor, in: Proceedings of NURETH-10, Seoul, Korea.
[12] W. Jaeger et al., Investigations of experiments with supercritical H_2O with the system code TRACE, in: Proceedings of NUTHOS-7, Seoul, Korea, 2008.
[13] K.H. Kang et al., Description of Freon Thermal Hydraulic Experimental Loop (FTHEL) and its Application, KAERI/TR-3592/2008, 2008.
[14] International Organization for Standardization (ISO), Guide to the Expression of Uncertainty in Measurement, ISBN 92-67-10189-9, 1995.
[15] K. Yamagata et al., Forced convection heat transfer to supercritical water flowing in tubes, Int. J. Heat Mass Transfer 15 (9) (1972) 2575–2593.
[16] R.A. Lee et al., Supercritical water heat transfer developments and application, in: Proceedings of Fifth International Heat Transfer Conference, Tokyo, Japan, 1974, pp. 335–339.
[17] I.L. Pioro et al., Experimental study on heat transfer to supercritical carbon dioxide flowing in a vertical tube, in: Proceedings of 13th International Conference on Nuclear Engineering (ICONE-13), Beijing, China, May 16–20, 2005.
[18] H.Y. Kim et al., Heat transfer test in a vertical tube using CO_2 at supercritical pressures, J. Nucl. Sci. Technol. 44 (3) (2007) 285–293.